



Long term friction: From stick-slip to stable sliding

Christophe Voisin,¹ François Renard,^{1,2} and Jean-Robert Grasso¹

Received 19 February 2007; revised 6 April 2007; accepted 24 May 2007; published 3 July 2007.

[1] We have devised an original laboratory experiment where we investigate the frictional behaviour of a single crystal salt slider over a large number of deformation cycles. Because of its physical properties, salt, an analogue for natural faults, allows for frictional processes plastic deformation and pressure solution creep to operate on the same timescale. During the same experiment, we observe a continuous change of the frictional behaviour of the slider under constant conditions of stiffness, temperature and loading velocity. The stick-slip regime is progressively vanishing, eventually reaching the stable sliding regime. Concomitantly, the contact interface, observed under the microscope, develops a striated morphology with contact asperities increase in length and width, arguing for an increase in the critical slip distance d_c . Complementary experiments including velocity jumps show that the frictional parameters of the rate and state friction law, a and b , progressively vanish with accumulated slip. The ultimate stage of friction is therefore rate and state independent under our experimental conditions. **Citation:** Voisin, C., F. Renard, and J.-R. Grasso (2007), Long term friction: From stick-slip to stable sliding, *Geophys. Res. Lett.*, 34, L13301, doi:10.1029/2007GL029715.

1. Introduction

[2] Macroscopic solid friction obeys simple empirical laws, known as Amontons-Coulomb friction laws [Amontons, 1699; Coulomb, 1785]. They state the existence of a static threshold in friction and that friction depends on the normal load and not on the apparent contact surface area. Secondary effects have been reported since these laws were first proposed. At rest, the static friction coefficient μ_s increases with the logarithm of time [Dieterich, 1972]. This increase is contemporary to the plastic deformation of microscopic contact asperities under stress [Dieterich and Kilgore, 1994]. When sliding has begun, friction drops to a dynamic level μ_d , which value is governed by the loading velocity and the material properties. The most complete description of friction is encapsulated in the empirical rate and state friction laws [Dieterich, 1979; Rice, 1983; Ruina, 1983]. These laws stipulate that friction depends on the slip velocity through two parameters a and b ; and on a state variable θ that accounts for a mean-field description of memory effects of the interface:

$$\mu = \mu_0 + a \ln(V/V_0) + b \ln(V\theta/d_c),$$

where μ_0 is a reference friction at V_0 ; V_0 is a reference velocity; V is the slider velocity; d_c is a critical slip distance,

akin to the mean size of asperities for instance. Experimental studies have shown the existence of a stable (a - b positive) and an unstable (a - b negative) sliding regime, the latter known as the stick-slip mode. The observation of one or other of these modes is reported to depend on the stiffness of the experimental apparatus and on the loading velocity [Dieterich, 1978, 1979; Heslot et al., 1994; Marone, 1998; Shimamoto, 1986]. As noticed by Shimamoto and Logan [1984], most of the empirical friction laws are based on short-term experiments and their extrapolation to the geological time scale (long term) is highly speculative because ductile processes (e.g. slow relaxation, pressure-solution, stress corrosion) are active within the upper crust [e.g., Gratier et al., 1999].

[3] In the following, we present results from friction experiments, original in two ways: (1) we use a monocrystal of salt, both brittle and ductile at the laboratory timescale; and (2) the evolving contact interface is observed under the microscope during deformation. We first describe the experimental apparatus. Second, we report on observations of a continuous change from stick-slip to stable sliding as slip accumulates under constant conditions of sliding velocity, normal load and temperature. Third, we show that the microstructure of the contact interface evolves from randomly rough to some striated morphology. This process of ageing, not observed in plastic or elastic multicontact friction experiments, is driven in our experiments by salt pressure solution creep (PSC). Complementary friction experiments show that the frictional parameters a and b are decreasing as the slip cumulates. Finally, we propose a physical interpretation to the transition from unstable to stable slip as controlled by the physico-chemical ageing of the initially rough sliding surface.

2. Experimental Method

[4] A cleaved monocrystal of halite (NaCl), roughened with sandpaper, is held under constant normal load and left in contact with a glass window (Figure 1). Salt is used because (1) it is transparent and allows for a direct observation of the contact interface; (2) it behaves both in a brittle and a ductile way at low stress at ambient temperature and humidity [Shimamoto, 1986]; and (3) the plastic deformations are effective over the duration of the friction experiments. Using a salt slider allows for the brittle and ductile deformation to be effective on the time scale of our experiments, aimed to serve as an analogue for natural faults deforming in the brittle and ductile regimes.

[5] The salt slider is mounted on an inverted microscope in order to observe the contact interface. Since halite is transparent, we image the contact asperities at the sliding surface using a high resolution camera located below the halite sample and focused at the slider interface undergoing shear. Doing so, we are able to track any visible deformation

¹Laboratoire de Géophysique Interne et Tectonophysique, CNRS, Observatoire de Grenoble, Université Joseph Fourier, Grenoble, France.

²Physics of Geological Processes, University of Oslo, Oslo, Norway.

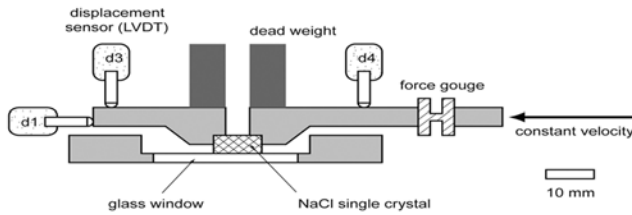


Figure 1. Schematic representation of the friction experiment. The 1 cm^2 surface area salt sample is housed in a plate made of a nickel iron alloy (Invar[®]) to limit thermal perturbations. A constant continuous velocity is imposed on the plate through a brushless motor. The maximum amount of slip is limited to 1.6 cm. The loading velocity can be reversed in order to achieve larger displacements. The frictional behaviour as well as its overall evolution is not affected when operating this way.

at the sliding surface. The slider is subjected to a constant normal load (1186,1g or 2651,4g) and is in contact with a glass or PMMA flat surface. Five displacement encoders record the plate movement in horizontal and vertical directions (LE/12/S IP50, Solartron). A force sensor (AEP TCA 5 kg) records the shear force exerted to move the slider (Figure 1). For all experiments the interface is subjected to ambient humidity. Under these conditions, a thin layer of water is adsorbed on the salt that promotes dissolution-crystallization reactions [Foster and Ewing, 2000]. A first set of experiments is conducted at constant velocity. A second set of experiments imposes velocity jumps to the slider in order to estimate the frictional parameters a and b . All experiments are gouge-free, conducted with bare roughened salt sliders.

3. A Continuous Change From Stick-Slip to Stable Sliding

3.1. Changes in the Frictional Behaviour of the Slider

[6] Figure 2a plots the continuous variation in slip of a salt slider against glass, from stick-slip to stable sliding over several hundreds of deformation cycles. At the beginning of the experiment, the slider experiences regular stick-slip oscillations with $35\ \mu\text{m}$ amplitude and 300 s waiting time (Figure 2b). The amplitude and waiting time gradually decrease as the slider enters the episodic stable sliding regime (Figures 2c, 2d, and 3a). The waiting time decreases from 300 s to 60 s after 500 cycles, while the slip amplitude decreases from $35\ \mu\text{m}$ to $10\ \mu\text{m}$. Most of this change occurs during the first 100 cycles. The process continues even when the stick-slip regime has disappeared and once the episodic stable sliding regime is established, with a decreasing period from 60 to 50 s and slip amplitude decreasing from 10 to $8\ \mu\text{m}$.

[7] The robustness of this change of frictional behaviour is tested with series of experiments conducted with different imposed velocity, initial roughness, and different materials in contact (see auxiliary materials).¹

3.2. Changes in the Contact Interface Roughness

[8] The change from stick-slip to stable sliding is concomitant with the ageing of the contact interface. The roughness of the slider surface is measured before and after the exper-

iment using white light interferometry (Figure 2a, colour insets). Initially, the surface root mean square (rms) of the roughness is close to $13.40 \pm 0.05\ \mu\text{m}$. Contact asperities are separated by grooves caused by the roughening process. Their mean size in width and length is about $30\ \mu\text{m}$. This initial surface is representative of a multicontact interface [Baumberger and Caroli, 2006]. By the end of the experiment, for a cumulated slip of 0.6 cm, the sliding surface exhibits a roughness rms of $7.80 \pm 0.05\ \mu\text{m}$. Contact asperities have grown and adopted an elongated shape in the direction of slip of dimensions 0.5 by 0.2 mm, giving the interface a striated morphology (Figure 2a, colour insets). The drastic change in surface morphology is accompanied by a downward vertical displacement of the slider. Inset in Figure 3 plots the power law relaxation of the vertical displacement with time. It is consistent with a deformation by pressure solution creep of the interface [Dysthe et al., 2002]. The emergence of a strongly anisotropic morphology cannot be explained by the elasto-plastic ageing of the contact interface that leads to an isotropic growth of the contact asperities [Berthoud et al., 1999; Dieterich and Kilgore, 1994]. The observed anisotropy arises from the coupling of pressure solution creep and horizontal displacement. Indeed, the change in topography is related to the development of the striated morphology of the contact interface. The matter dissolved from each contact area precipitates in the stress shadow of each asperity, leading to the observed anisotropic pattern.

3.3. Changes in Frictional Parameters a and b

[9] The two parameters a and b measure the velocity dependence of friction and the increase of static friction with hold time [Dieterich, 1979]. The difference $(b-a)$ whenever positive implies a velocity weakening behavior, leading to stick-slip as observed at the beginning of our experiments. We conducted a series of experiments with velocity cycles (jumps from 1 to $10\ \mu\text{m/s}$) in order to measure these secondary effects of friction. Figure 3b plots three measures of a and b , for different cumulated slips. Both parameters are markedly decreasing with the cumulated slip. After a few centimeters of slip, the velocity jumps are hardly noticeable in the frictional behavior. During this final stage, the change in friction with velocity, if any, is insignificant. Therefore we cannot resolve whether the $(b-a)$ difference changes sign. The slider has evolved from velocity weakening to velocity neutral.

[10] Velocity stepping experiments may be used to infer the value of d_c [Dieterich, 1979; Dieterich and Kilgore, 1994]: it is defined as the width of the direct friction effect pulse. In the experiment presented in Figure 3b, the estimate of d_c gives a $22.34 \pm 5.86\ \mu\text{m}$, in accordance with the mean size of asperities of the initial contact interface. However, because the direct friction effect disappear after some accumulated slip, the measure of d_c is no more possible. We have to rely on the direct observation of the contact interface and on the mean size of contact asperities as a proxy to d_c .

4. Interpretation

[11] Stick-slip and episodic stable sliding modes are described in the rate and state friction framework [Dieterich,

¹Auxiliary material data sets are available at <ftp://ftp.agu.org/apend/gl/2007gl029715>. Other auxiliary material files are in the HTML.

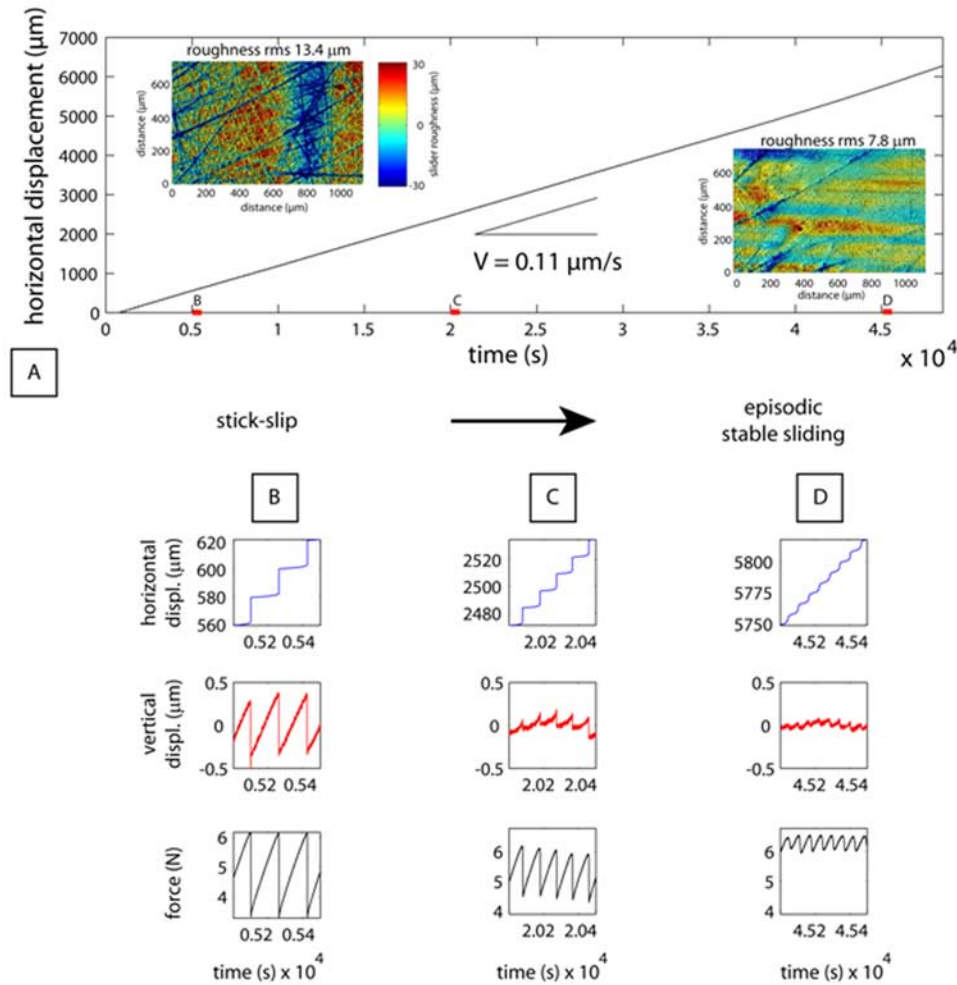


Figure 2. (a) Change in frictional behavior of a salt/glass friction experiment (loading velocity: $0.11 \mu\text{m/s}$; normal load: 0.26 MPa). The slider exhibits regular stick-slip at the beginning with a jump amplitude of about $35 \mu\text{m}$ and a waiting time of about 300 s . At the end of the experiment, the slider exhibits an episodic stable sliding behavior with small oscillations of its speed around the imposed velocity. Color insets represent the topography of the frictional interface before and after the experiment measured by white light interferometry, with a roughness resolution of $0.05 \mu\text{m}$ (Wyko 2000 Surface Profiler from Veeco). (b) The beginning of the experiment. The accumulated slip is about $500 \mu\text{m}$. The stick-slip behavior is clearly recorded both in horizontal and vertical displacements. Amplitudes are of the order of $20 \mu\text{m}$ and $0.3 \mu\text{m}$ in horizontal and vertical directions respectively. Long phases of stress build-up are followed by rapid force drops of up to 3 N as the slider moves abruptly. (c) The mid-run of the experiment, with a cumulated slip of $2500 \mu\text{m}$. The stick-slip behavior is still recorded. Horizontal and vertical jumps are visible with amplitudes of about $10 \mu\text{m}$ and $0.1 \mu\text{m}$ respectively. The stress drops are about 2 N . (d) The end of the experiment, with a cumulated displacement of about $6000 \mu\text{m}$. Smooth oscillations typical of the episodic stable sliding regime are recorded. Note that the mean force that has to be exerted for the slider to move has increased: the friction coefficient has increased and the contact interface has strengthened. This is consistent with the increase of the real area of contact.

1979]. At constant driving velocity, the occurrence of one or other of these two frictional behaviors is related to a simple condition on the stiffness K of the experimental apparatus [Heslot *et al.*, 1994; Scholz, 2002]. To ensure stick-slip oscillations, one must have first $a < b$; second, K must obey the following relation:

$$K < K_c = W \cdot (b-a)/d_c \quad (1)$$

W stands for the normal load exerted on the slider, including its own mass. d_c stands for a length scale typical of the interface, e. g. the mean size of asperities. Equation (1) arises

from a stability analysis of a slider block under rate and state friction law [Rice and Ruina, 1983] and defines the value of the critical stiffness K_c below which stick-slip oscillations do exist. Changes from stick-slip to episodic stable sliding are reported in various conditions. Changes in the driving velocity, in the stiffness or in the normal load all affect the frictional behavior [Heslot *et al.*, 1994]. The presence of a developed gouge also affects the occurrence of stick-slip or stable sliding by changing the $(b-a)$ value [Beeler *et al.*, 1996; Marone *et al.*, 1990]. Finally, temperature changes also affect the value of $(b-a)$ [Scholz, 1998].

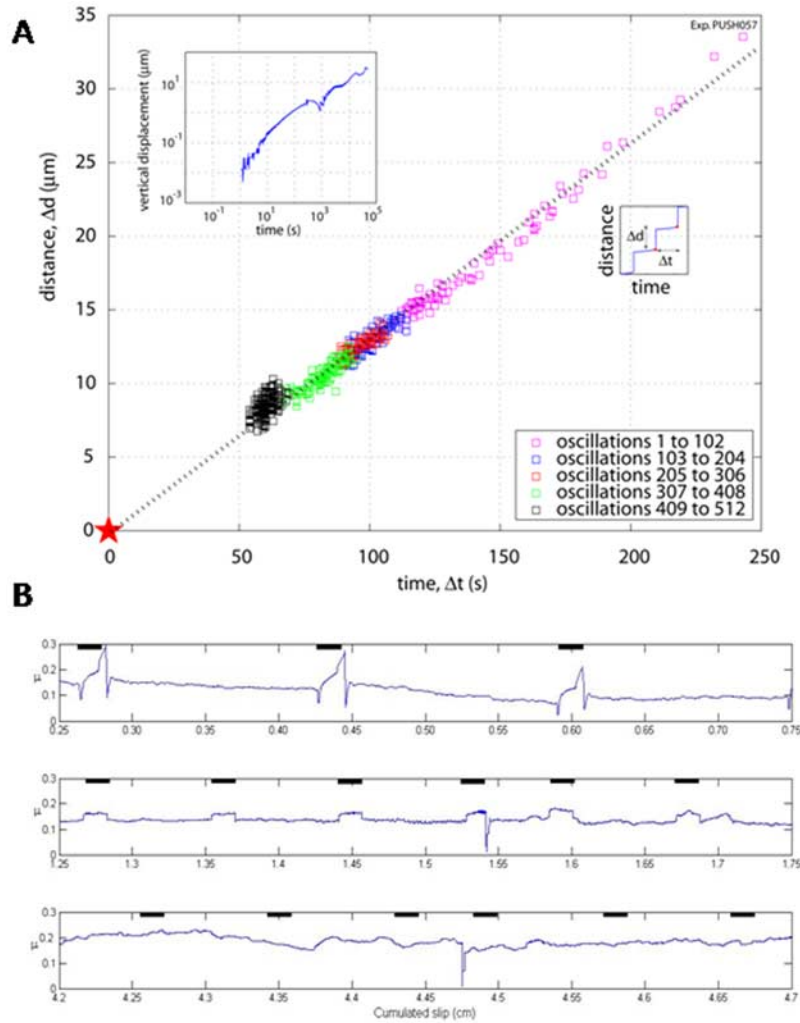


Figure 3. (a) Stick-slip amplitude (Δd) versus waiting time (Δt) for the friction experiment PUSH057. Color codes for increasing time: magenta, blue, red, yellow, and black. A clear trend to a decrease in amplitude and waiting time arises from the data. All control parameters being constant, the spreading of data characterizes the morphological change of the interface. The red star (left lower corner) indicates the final state to be reached by the slider: the slider moves at the exact imposed velocity. The inset shows the settlement of the slider during the experiment, consistent with the PSC deformation of the interface. Second-order oscillations corresponding to stick-slip events also decrease with time. (b) Velocity jump experiments for a , b , and d_c estimates. The slider is submitted to velocity cycles (1 and 10 $\mu\text{m/s}$). The black rectangles indicate the periods of slow velocity. The three lines correspond to three exerts of an experiment (constant conditions of normal stress and temperature – no gouge development) taken at different times and cumulated displacement. Sudden drops in friction observed at 1.53 and 4.5 cm corresponds to change in the direction of slip. Line 1: the direct friction effect (related to a) and the slow relaxation (related to b) are visible. Estimates of a , b , and d_c are: 0.1209 ± 0.0094 , 0.26 ± 0.0296 , and $22.33 \pm 5.86 \mu\text{m}$ respectively. Line 2: the direct friction effect has disappeared. Estimates of a and d_c following the methodology of *Dieterich and Kilgore* [1994] are not appropriate. The change in velocity induces an immediate change in friction ($b = 0.0862 \pm 0.0252$) that is also decreasing in amplitude with the cumulated displacement. Line 3: the change in friction is no more visible. The slider has become velocity neutral.

[12] Our experiments are conducted under constant conditions of velocity, mass, stiffness and temperature. The low velocities we use preclude the wear of the slider and the development of a gouge. We must seek for other explanations to the observed transition from stick-slip to stable sliding. Since the normal load W is kept constant throughout the experiments, equation (1) implies that K_c has to decrease in order to explain the observed change from stick-slip to

stable sliding. Our two observations, namely (1) the $(b-a)$ decrease with time and (2) the contact asperity size increase with time, both contribute to such a K_c decrease with the accumulated slip. The direct observation of topography changes on the frictional interface (Figure 2a), akin to the growth of contact asperities, supports an increase in d_c with time, that is a decrease in K_c . This increase in d_c also implies a stabilization of the slider because of its finite size. Indeed,

as d_c increases the nucleation length increases as well, presumably up to the stability limit [Dascalu et al., 2000; Voisin et al., 2002]. In the conditions of the experiment, the increase in d_c is related to changes in the geometry of contact asperities, the latter being driven by PSC. This mechanism is solely responsible for a fast evolution of the interface under the low normal and shear stress conditions of our experiments [Gratier, 1993; Karcz et al., 2006].

[13] Although our experiments are performed under constant conditions of temperature and normal stress, and with no gouge, changes in $(b-a)$ do occur. Indeed, the value of $(b-a)$ approaches zero as both a and b vanish. The immediate consequence is that $K_c \rightarrow 0$ as slip accumulates. Since $(b-a) = \partial\mu/\partial(\ln V)$, the ultimate frictional behavior of the salt slider is rate independent (Figure 3b). A second consequence arises from the definition of b : $b = \partial\mu/\partial \log t$. Since $b \rightarrow 0$ as the slip cumulates, it implies that μ does not increase anymore at rest. The ultimate frictional behavior of the salt slider is state independent.

[14] We explain the change from stick-slip to stable sliding as a progressive decrease in K_c with the cumulative slip. Changing the stiffness of the experiment K will not preclude this evolution to occur. Indeed since $K_c \rightarrow 0$ with the cumulative slip, the change from stick-slip to stable sliding would be observed whatever the stiffness of the experiment. This hypothesis will be the concern of a future work.

5. Conclusion

[15] The frictional behaviour of a single crystal salt slider is investigated under constant conditions of normal load, driving velocity, and temperature. We observe a progressive change from stick-slip to stable sliding with accumulative displacement. During the experiment, all frictional parameters are evolving: a and b are decreasing while d_c is increasing. These changes are contemporary to the morphological evolution of the contact interface, i.e. the development of a striated pattern driven by the coupling of PSC and slip. The increase in d_c and the decrease in $(b-a)$ both lead to the progressive vanishing of K_c , the critical stiffness for stick-slip. The salt slider is therefore forced to a mode of stable sliding, with no more rate and state dependence.

[16] **Acknowledgments.** We thank P. Giroux, R. Guiguet, A.-M. Boullier, and L. Jenatton for their help in designing the experiment; D. Dysthe, J. Feder, D. Brito, J.-P. Gratier, L. Margerin, I. Manighetti, A. Helmstetter, and K. Mair for thoughtful discussions. We acknowledge grants from CNRS (ATI, Dyeti) and from Université Joseph Fourier (BQR).

References

- Amontons, G. (1699), De la résistance causée dans les machines, *Mém. Acad. R. Sci.*, 206–226.
- Baumberger, T., and C. Caroli (2006), Solid friction from stick-slip down to pinning and aging, *Adv. Phys.*, 55(3–4), 279–348.
- Beeler, N. M., et al. (1996), Frictional behavior of large displacement experimental faults, *J. Geophys. Res.*, 101, 8697–8715.
- Berthoud, P., et al. (1999), Physical analysis of the state- and rate-dependent friction law: Static friction, *Phys. Rev. B*, 59(22), 14,313–14,327.
- Coulomb, C. A. (1785), Théorie des machines simples, *Mém. Math. Phys. Acad. Sci.*, 10, 161–331.
- Dascalu, C., et al. (2000), Fault finiteness and initiation of dynamic shear instability, *Earth Planet. Sci. Lett.*, 177(3–4), 163–176.
- Dieterich, J. H. (1972), Time dependent friction in rocks, *J. Geophys. Res.*, 77, 3690–3697.
- Dieterich, J. H. (1978), Time dependent friction and the mechanics of stick-slip, *Pure Appl. Geophys.*, 116(4–5), 790–806.
- Dieterich, J. H. (1979), Modeling of rock friction: 1. Experimental results and constitutive equations, *J. Geophys. Res.*, 84, 2161–2168.
- Dieterich, J. H., and B. D. Kilgore (1994), Direct observation of frictional contacts: New insights for state-dependent properties, *Pure Appl. Geophys.*, 143(1–3), 283–302.
- Dysthe, D. K., et al. (2002), Universal scaling in transient creep, *Phys. Rev. Lett.*, 89(24), 246102.
- Foster, M. C., and G. E. Ewing (2000), Adsorption of water on the NaCl (001) surface: II. An infrared study at ambient temperatures, *J. Chem. Phys.*, 112(15), 6817–6826.
- Gratier, J.-P. (1993), Experimental pressure solution of halite by an indenter technique, *Geophys. Res. Lett.*, 20, 1647–1650.
- Gratier, J.-P., et al. (1999), How pressure solution creep and fracturing processes interact in the upper crust to make it behave in both a brittle and viscous manner, *J. Struct. Geol.*, 21(8–9), 1189–1197.
- Heslot, F., et al. (1994), Creep, stick-slip, and dry-friction dynamics: Experiments and a heuristic model, *Phys. Rev. E*, 49(6), 4973–4988.
- Karcz, Z., et al. (2006), Stability of a sodium chloride indenter contact undergoing pressure solution, *Geology*, 34(1), 61–63.
- Marone, C. (1998), Laboratory-derived friction laws and their application to seismic faulting, *Annu. Rev. Earth Planet. Sci.*, 26, 643–696.
- Marone, C., et al. (1990), Frictional behavior and constitutive modeling of simulated fault gouge, *J. Geophys. Res.*, 95, 7007–7025.
- Rice, J. R. (1983), Constitutive relations for fault slip and earthquake instabilities, *Pure Appl. Geophys.*, 121(3), 443–475.
- Rice, J. R., and A. L. Ruina (1983), Stability of steady frictional slipping, *J. Appl. Mech.*, 50(2), 343–349.
- Ruina, A. (1983), Slip instability and state variable friction laws, *J. Geophys. Res.*, 88, 359–370.
- Scholz, C. H. (1998), Earthquakes and friction laws, *Nature*, 391(6662), 37–42.
- Scholz, C. H. (2002), *The Mechanics of Earthquake and Faulting*, 496 pp., Cambridge Univ. Press, Cambridge, U. K.
- Shimamoto, T. (1986), Transition between frictional slip and ductile flow for halite shear zones at room-temperature, *Science*, 231(4739), 711–714.
- Shimamoto, T., and J. M. Logan (1984), Laboratory friction experiments and natural earthquakes: An argument for long-term tests, *Tectonophysics*, 109(3–4), 165–175.
- Voisin, C., et al. (2002), Process and signature of initiation on a finite fault system: A spectral approach, *Geophys. J. Int.*, 148(1), 120–131.
- J.-R. Grasso, F. Renard, and C. Voisin, Laboratoire de Géophysique Interne et Tectonophysique, CNRS, BP 53, F-38041 Grenoble, France. (cvoisin@obs.ujf-grenoble.fr)